Postharvest Biology and Technology 112 (2016) 75–86

Contents lists available at ScienceDirect

Postharvest Biology and Technology

journal homepage: www.elsevier.com/locate/postharvbio

Metabolite and transcriptomic analysis reveals metabolic and regulatory features associated with Powell orange pulp deterioration during room temperature and cold storage

Ning Tang, Wei Deng, Nan Hu, Nan Chen, Zhengguo Li*

Genetic Engineering Research Center, School of Life Sciences, Chongqing University, Chongqing 400030, China

ARTICLE INFO

Article history:
Received 23 June 2015
Received in revised form 22 September 2015
Accepted 14 October 2015
Available online 28 October 2015

Keywords:
Powell orange
Pulp deterioration
Transcriptome
Metabolite
Room-temperature storage
Low-temperature storage

ABSTRACT

Fruit senescence is an inevitable developmental process that involves dynamic alterations in many metabolic and regulatory pathways. In this study, GC–MS and RNA-Seq were employed to characterize the metabolite and transcriptomic profiles during postharvest storage under room temperature (RT) and low temperature (LT) in Powell (*Citrus sinensis*) fruits. Results showed that RT-storage up-regulated genes involved in primary metabolism including sucrose metabolism, glycolysis, gluconeogenesis, fermentation and GABA shunt pathways, resulting in declines of sucrose and organic acids such as malate, citrate and α-ketoglutaric acid, and accumulations of hexoses and GABA. Furthermore, calcium-sensor proteins were strongly induced including *CMLs*, *CBL-CIPKs* and *CPKs*, indicating the potential roles of calcium signaling during postharvest storage under RT. RT-storage enhanced ABA and ethylene signaling pathways via up-regulation of *PYLs*, *ABI5* and *ERFs*, which revealed hormone regulatory networks on fruit senescence. In addition, the induced *RPLs*, *NAC* and *WRKY* transcription factors and *MAP kinases* provided a comprehensive view on the fruit senescence regulation. During LT storage, the levels of metabolites and catabolism related genes were substantially maintained, and auxin signal was modulated by upregulation of *TIR1* and downregulation of *Aux/IAAs*. In summary, RT storage accelerates calcium, ABA and ethylene signals, which could positively regulate fruit senescence and result in induced primary metabolism and fruit quality deterioration. LT storage might accelerate the auxin signal, thus delaying senescence and maintaining fruit quality.

1. Introduction

Citrus is one of the most important fruits in world trade due to its high nutritional quality and pleasant flavor. Citrus fruit is a complex matrix that contains several groups of metabolites such as sugars, organic acids, amino acids, volatiles, phenolics, carotenoids and vitamins, which are essential factors responsible for its commercial viability (Cerdán-Calero et al., 2012). During postharvest storage at ambient temperature, senescence, as an inevitable and negative biological process, is characterized by a general reduction in biochemical and physiological functions (Paliyath et al., 2009), which follows the rapid deterioration of fruit quality in terms of nutrient composition, flavor, and sensory acceptability (Tietel et al., 2011). Hence, the knowledge of quantitative profiling for these metabolites is of major importance for biomarkers discovery during postharvest fruit senescence and has significant implications for our food supply, nutrition, and health.

Fruit senescence is the final step of fruit development, during which cells undergo a major functional transformation from carbon assimilation and other anabolic reactions to degradation of macromolecules such as proteins, lipids, and nucleic acids that results in cell dysfunction, structural disintegration and cell death (Buchanan-Wollaston, 1997; Yun et al., 2012). These dynamic processes involve a series of molecular changes under gene regulation in response to developmental and environmental cues (Osorio et al., 2012). To better understand fruit senescence mechanisms during postharvest, several studies have been focused on transcript and metabolite levels in peels and pulps of citrus fruits, such as mandarins (Matsumoto and Ikoma, 2012; Tietel et al., 2011), Hirado Buntan Pummelo (Sun et al., 2013; Yun et al.,

Abbreviations: CIPK, CBL-interacting protein kinase; CMLs, calcium-binding proteins; CPK, calcium-dependent protein kinase; DGEs, differentially expressed genes; FDRs, false discovery rates; GABA, γ-aminobutyrate; GC–MS, gas chromatography–mass spectrometry; HSPs, heat shock proteins; qRT-PCR, quantitative real-time PCR; RPLs, ribosomal proteins; RNA-Seq, RNA sequencing.

* Corresponding author. Fax: +86 23 6512 0483.
E-mail addresses: sabrina-0810@hotmail.com (N. Tang), dengwei1977@cqu.edu.cn (W. Deng), hunan.1210@163.com (N. Hu), chennan0205@gmail.com (N. Chen), zhengguoli@cqu.edu.cn (Z. Li).

http://dx.doi.org/10.1016/j.postharvbio.2015.10.008
0925-5214/

2012), Ponkan (Chen et al., 2012) and Olinda Valencia orange (Ma et al., 2014).

Transcriptome analysis revealed that these processes including primary and secondary metabolism, as well as the regulations mediated by plant hormone or other signals, were significantly altered during postharvest storage (Tietel et al., 2011; Yun et al., 2012). The most well-studied primary metabolism could be the investigations of the changes in sugars, organic acids and amino acids, which are the important components of fruit quality determinants (Matsumoto and Ikoma, 2012). However, the profiles of these metabolites showed different patterns in previous studies, which varied depending on cultivars, temperatures, pre-treatments and duration of storage (Chen et al., 2012; Matsumoto and Ikoma, 2012; Sun et al., 2013; Yun et al., 2012). Sugars and organic acids are regarded as the metabolic resources required for construction of the carbon skeleton and energy supply in plants (Sun et al., 2013; Wu et al., 2014). Meanwhile, amino acids are thought to be involved in flavor formation and adaptation in response to abiotic stresses (Matsumoto and Ikoma, 2012). Besides, sugars may serve as important signals that regulate various processes in plant development. There is compelling evidence on the crosstalk between sugar and hormone signaling pathways, that creates a positive interaction between auxin, but antagonistic relationships with ABA and ethylene (Liu et al., 2013). In general, the pathways related to biosynthesis and catabolism of these metabolites, such as sucrose metabolism, glycolysis, TCA cycle and other pathways, were dramatically regulated during postharvest fruit senescence. Therefore, integration of gene expression and metabolite composition data during postharvest storage can give important insights into the transcriptional regulation of metabolism associated with fruit senescence. With regard to regulatory factors, calcium involved in regulation of fruit ripening process and postharvest senescence. As an important mineral element, calcium regulates fruit quality through participating in cell wall structure and maintaining fruit firmness (Aghdam et al., 2012). Recently, it has been reported calcium binding proteins (CaBPs) and calcineurin B-like proteins (CBLs) were strongly altered during postharvest storage, suggesting the pivotal roles of calcium signaling in fruit senescence (Jiang et al., 2014; Yun et al., 2012). Several plant hormones, such as ABA, ethylene and auxin, are involved in the process of fruit senescence. Sun et al. (2010) showed that ABA was increased by *VvNCED1* up-regulation, a key enzyme for ABA biosynthesis, and ABA accumulation will initiate the onset of berry senescence during postharvest periods of berries. Traditionally, fruit senescence at the molecular level in climacteric fruits is regulated by ethylene (Cara and Giovannoni, 2008). It is controversial whether ethylene is involved in fruit development and senescence in non-climacteric fruits such as citrus. Porat et al. (1999) found that exogenous ethylene had disadvantageous effects on several postharvest parameters, which increased the appearance of chilling injury symptoms, stem-end rot decay, and the content of volatile off-flavors in the juice. However, no ethylene-related proteins/genes were significantly altered during postharvest storage in Hirado Buntan Pummelo (Yun et al., 2012). Furthermore, transcription factors also play a key role in regulating both senescence and hormone signaling. A previous study showed that 2,4-D retarded fruit senescence by up-regulating defense-related transcriptional factors, mainly AP2/ERF, WRKY, and NAC family members (Ma et al., 2014).

Although some regulatory genes related to fruit senescence during postharvest storage has been characterized by transcriptomic approaches in the previous studies (Ma et al., 2014; Yun et al., 2012), there is little information on how these genes function in the global control of the process. Powell is a late-ripening navel orange, which reaches legal maturity around mid-March in Chongqing, China. It is susceptible to ambient temperature (room temperature, RT) since the weather gets warmer after harvest. Low temperature (LT) storage is extensively used to extend storage life and maintain fruit quality during postharvest storage. In the present study, transcriptomic and metabolomic approaches were performed to characterize the dynamic changes of metabolites and fundamental regulatory pathways under RT and LT storage during postharvest in citrus, which might help to unravel the global picture of fruit senescence regulatory networks.

2. Materials and methods

2.1. Plant materials

Powell orange (*Citrus sinensis* (L.) Osb.) fruits at commercial ripening stage were harvested from a local orchard located in Fengjie, Chongqing, China. The fruits of uniform size and color were divided randomly into two groups. One group was held in room conditions at 25 °C and 60–70% RH, and another group was stored at 5 °C and 85–90% RH. Fruit samples were collected at 30, 60 and 90 DAH and the fruits with 0 days of storage were set as control. In brief, fruits were washed and sliced into halves longitudinally, and then juice sacs and juices were obtained from each section. Juices were collected using a manual extractor, sieved through gauze. All the samples were frozen in liquid nitrogen immediately and stored at −80 °C until analysis.

2.2. GC–MS analysis of polar metabolites

400 μL juice was transferred into a glass vial, followed by adding 20 μL ribitol (0.2 mg/mL) as an internal standard, and then the mixture was dried by nitrogen blowing instrument. 80 μL methoxamine hydrochloride solutions (15 mg/mL, in pyridine) was emptied into the dried samples and then the glass vial was vortexed and incubated at 37 °C for 90 min. After that, trimethylsilylation was performed by inpouring 80 μL of BSTFA (with 1% TMCS) and heating at 70 °C for 1 h. The resulting mixture was used as a GC–MS analysis sample. Polar metabolites were determined in six replicates.

GC–MS was performed by Agilent 7890A GC/5975C MS system, equipped with an Agilent J&W Scientific HP-5MS capillary column (5% phenyl/95% methylpolysil-oxane, 30 m × 250 μm i.d.). The GC–MS parameters were as follows. Oven temperature ramp were 70 °C for 2 min, 10 °C/min ramp up to 140 °C, then 4 °C/min ramp up to 240 °C, finally heating at 10 °C/min until 300 °C and held for 8 min. Helium was used as carrier gas at constant flow of 1.0 mL/min. The injector temperature was held at 270 °C and a volume of 1 μL was injected with splitless. The EI ion source temperature was kept at 230 °C and the quadrupole temperature was kept at 150 °C. Mass spectra and TIC were acquired over the mass range m/z 50–600.

For identification and relative quantification of metabolites, the resulting high-throughput chromatography data files are typically processed via R software (http://cran.r-project.org/) and TagFinder. Each individual peak areas of compounds were integrated. Relative abundance was represented by the normalized peak area. That was, the peak area ratio of each compound to a corresponding internal standard was calculated as the response. To identify the differentially expressed metabolites, the Student's t-test and variable influence on projection (VIP) values were employed to determine statistical significance. Differences were considered to be significant when $P < 0.05$ and VIP > 1. Finally, the compound was identified by comparing the MS with those in NIST 2005 Mass Spectral library.

2.3. Analysis of ethanol and acetaldehyde by GC

The concentration of ethanol and acetaldehyde were conducted by headspace gas chromatography with flame ionization detection (GC–FID). 5 mL of juice was poured into a 22 mL headspace vial and capped with a Teflon septum. The Vials were incubated at 70 °C for 25 min. GC analysis was performed on an Agilent7890A GC coupled with 7693 autosampler (Agilent technologies, Santa Clara, CA, USA). An Agilent DB-WAX column (30 m × 0.32 mm × 0.25 μ) was used. Vial temperature, loop temperature and transfer line temperature were fixed to 70 °C, 80 °C and 90 °C, respectively. The oven temperature was initially set at 50 °C for 5 min, 10 °C/min up to 100 °C, and then 30 °C/min until 150 °C. The injector and FID temperature were operated at 150 °C and 220 °C, respectively. The volume of injection was 1.0 μL, with a split ratio of 20. The concentrations were calculated based on peak area measurements. All metabolites were analyzed in triplicate.

2.4. RNA extraction and Illumina sequencing

Total RNA from citrus pulp was extracted and purified using QIAGEN RNeasy Plant Mini Kit and RNase-free DNase set (QIAGEN, Germany) according to manufacturer's handbook. RNA-Seq was performed at Shanghai Majorbio Biopharm Technology Co., Ltd. (Shanghai, China). A TruSeq™ RNA Sample Preparation Kit (Illumina, Inc.) was employed to construct cDNA library. Briefly, poly(A) mRNA was enriched from 5 μg total RNA via oligo(dT) magnetic beads and cleaved using divalent cations. Double-stranded cDNA was generated and processed with end-repair, A-tailed and adapters ligation. Then the products enriched by PCR amplification were purified through 2% agarose gel electrophoresis and quantified by TBS380 (Picogreen). cDNA libraries was subsequently sequenced using Illumina HiSeq™ 2000 platform.

2.5. Analysis of RNA-Seq data

The Raw sequences were filtered by removing the adapter sequences using SeqPrep (https://github.com/jstjohn/SeqPrep). Deteriorate quality bases at the end were trimmed using sickle (https://github.com/najoshi/sickle). Reads less than 20 bp after processing were discarded. To identify the gene expression signatures from the citrus libraries, the orange (*C. sinensis*) genome database (http://citrus.hzau.edu.cn/) was used as a reference database. All clean reads were aligned to the reference sequences using Tophat (http://tophat.cbcb.umd.edu/) with default parameters (Trapnell et al., 2009). To identify differentially expressed genes (DEGs) between the samples, transcript abundance was estimated using the fragments per kilobase of exon per million mapped reads (FRKM) method (Trapnell et al., 2010). Cuffdiff software (http://cufflinks.cbcb.umd.edu/) was applied to calculate gene expression and infer isoforms quantification (Trapnell et al., 2013). A *P*-value could denote its expression difference between two samples, and false discovery rates (FDRs) were used to determine the threshold of *P* value. FDR ≤ 0.05 and log 2 ratio ≥ 1 were considered statistically significant.

2.6. Validation of RNA-seq data by quantitative real-time PCR

cDNA was synthesized from 1 μg of total DNA-free RNA using RevertAid First Strand cDNA Synthesis Kit (Fermentas, USA) according to the manufacturer's instruction. Gene-specific primers for selected genes were designed by online software (https://www.genscript.com/ssl-bin/app/primer) (Supplementary Table S1) and melt curve analysis was used to confirm the specificity. Quantitative real-time PCR (qRT-PCR) were carried out using Fast SYBR Mixture (CWBIO, Beijing) on an Bio-Rad CFX connect real-time PCR detection system by the two-step method, which was incubated at 95 °C for 10 min, then followed by 40 cycles of 95 °C for 15 s, 60 °C for 60 s. For all qPCR experiments, three biological replicates were performed. Relative expression levels were calculated based on the $2^{-\Delta\Delta Ct}$ method using actin as reference gene.

Supplementary material related to this article found, in the online version, at http://dx.doi.org/10.1016/j.postharvbio.2015.10.008.

3. Results and discussion

3.1. Metabolic changes in Powell fruit during postharvest storage process

To reveal physiological mechanisms during postharvest process, metabolic changes in RT- and LT-storage were analyzed by GC–MS in the current study. A total of 25 primary metabolites (6 sugars, 5 organic acids, 13 amino acids and 1 other compound) were identified and quantified relatively (Supplementary Table S2). Principal Component analysis (PCA) demonstrated that fruit samples stored for 60 and 90 days at room temperature separated clearly from control samples along PC1($R^2X = 0.639$, $Q^2 = 0.541$) (Fig. 1A), indicating differences in primary metabolites after RT storage. Accordingly, the clusters of the LT-stored fruit

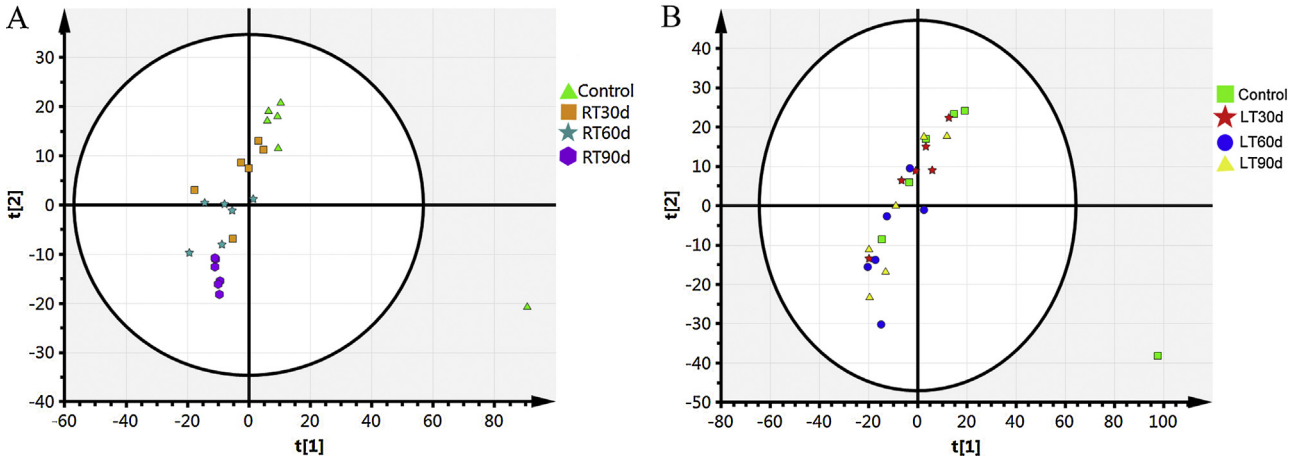

Fig. 1. Principal component analysis (PCA) of primary metabolites determined by GC–MS. PCA score plots (*t*[1] vs *t*[2]) for the first two principal components during postharvest storage under RT(A) and LT(B) for 90 days. Each sample was marked using individual symbol and color in RT group and LT group, respectively. 6 biological replicates were performed.

Table 1
The differential metabolites identified in Powell fruit juices by GC–MS during postharvest storage.

Retention time	Compounds	Fold (log_2 ratio)			
		RT30d/0d	RT60d/0d	RT90d/0d	LT90d/RT90d
	Sugars				
16.86	D-Fructose	–	0.360	0.435	-0.253
17.24	D-Glucose	–	0.726	1.426	-0.716
17.31	D-Galactose	–	0.372	0.4322	-0.228
18.85	*Myo*-inositol	–	0.325	0.278	-0.218
23.57	Sucrose	–	-0.618	-0.758	0.548
	Organic acids				
12.32	Malic acid	–	−0.287	−0.797	0.711
13.25	α-Ketoglutaric acid	–	−1.339	−1.126	0.801
16.10	Citric acid	–	−0.354	−0.403	–
	Amino acids				
12.79	γ-Aminobutyrate (GABA)	–	1.154	1.029	−1.304

"–" represents that no significant changes were observed.

samples and control groups overlapped ($R^2X = 0.577$, $Q^2 = 0.498$) (Fig. 1B), and no remarkable changes in metabolic profiles were observed in the duration of LT-storage. Nine metabolites were identified to be altered significantly during RT storage phase (Table 1). The sugars including D-fructose, D-glucose, D-galactose and *myo*-inositol were remarkably increased at 60 and 90 days after harvest, whereas sucrose displayed an outstanding decrease. The contents of malic acid, citric acid and α-ketoglutaric acid were reduced conspicuously. We also found an amino acid, γ-aminobutyrate (GABA), showing extremely higher levels after lengthy storage. Compared to RT-storage, there were 2 metabolites with significant accumulation and 5 with dramatic reduction at 90 days after harvest under LT-storage (Table 1). Overall, metabolic profiling identified the altered metabolites during RT long-term storage, while LT-storage can obviously maintain the levels of metabolites in fruits.

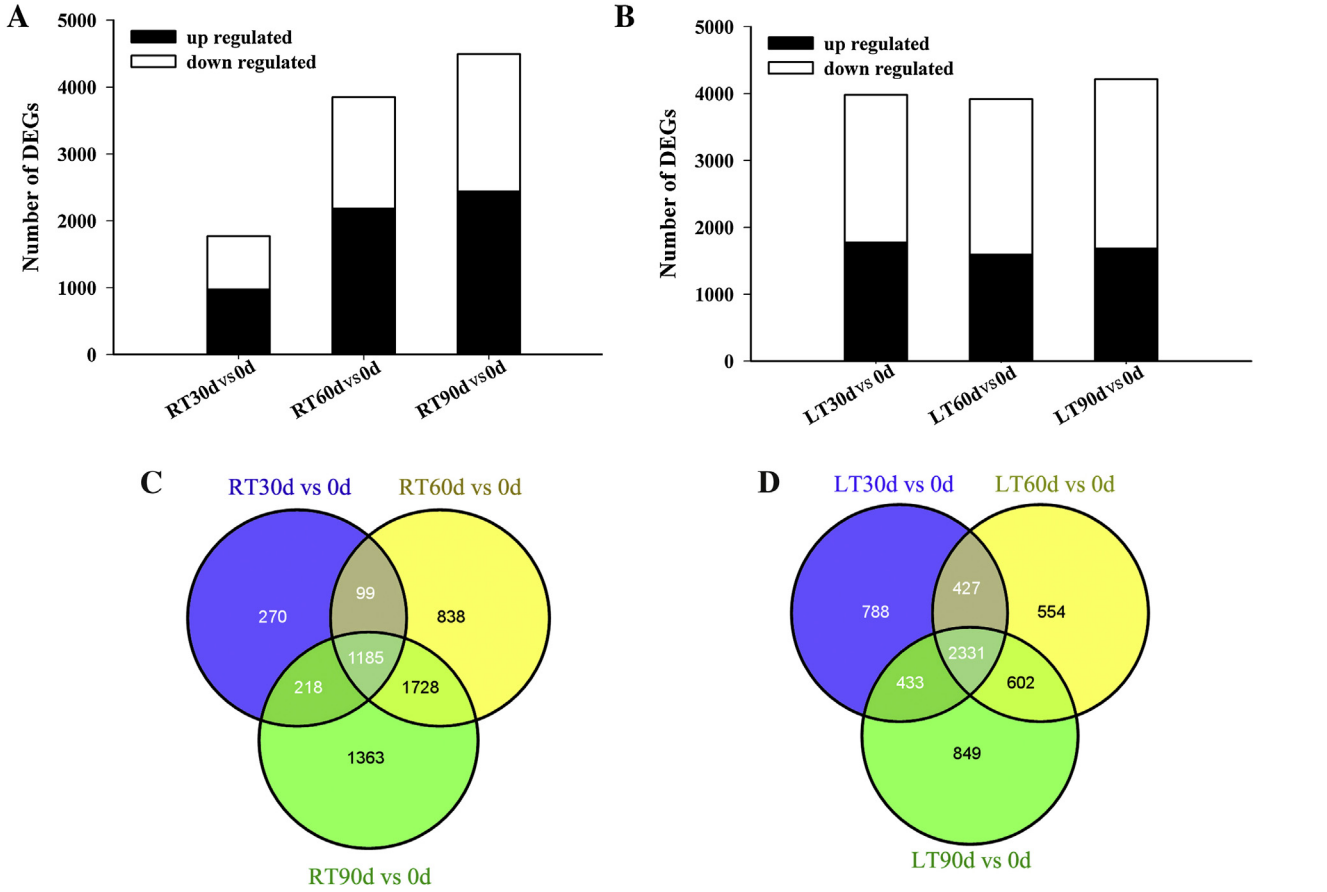

Fig. 2. DEGs identified by transcriptome analysis during postharvest storage of Powell fruits.
With respect to control, number of genes differentially expressed at 30, 60 and 90 days after harvest under RT(A) and LT (B). The two adjacent sets of bars represent the up-regulated (black) and down-regulated (white) genes, respectively.
Venn diagram shows the overlap/non-overlap of DEGs at 30, 60 and 90 days after harvest under RT(C) and LT (D) storage.

Supplementary material related to this article found, in the online version, at http://dx.doi.org/10.1016/j.postharvbio.2015.10.008.

3.2. Transcriptome profiling of Powell fruits during postharvest storage process

The pulps of Powell fruits at different storage periods and temperatures were used for RNA-Seq analysis. A total of 5701 and 5984 genes were differentially expressed under RT and LT storage, respectively, compared with those in the control (Supplementary Table S3). The number of DEGs was increased gradually with increasing storage time under RT (Fig. 2A), whereas it substantially remained constant at the duration of LT storage (Fig. 2B), which is in accordance with the fact that LT can maintain fruit quality. Among these DEGs, 1185 and 2331 were consistently differentially expressed throughout 90-days storage under RT and LT, respectively (Fig. 2C and D).

Supplementary material related to this article found, in the online version, at http://dx.doi.org/10.1016/j.postharvbio.2015.10.008.

To validate the accuracy of the RNA-Seq data, we selected 17 genes and investigated their transcript levels using qRT-PCR (Fig. 3A–S). There was a good correlation ($R^2 = 0.87$, $P < 0.001$) between the two methods (Fig. 3T), indicating the high reliability of the RNA-Seq data obtained in our study.

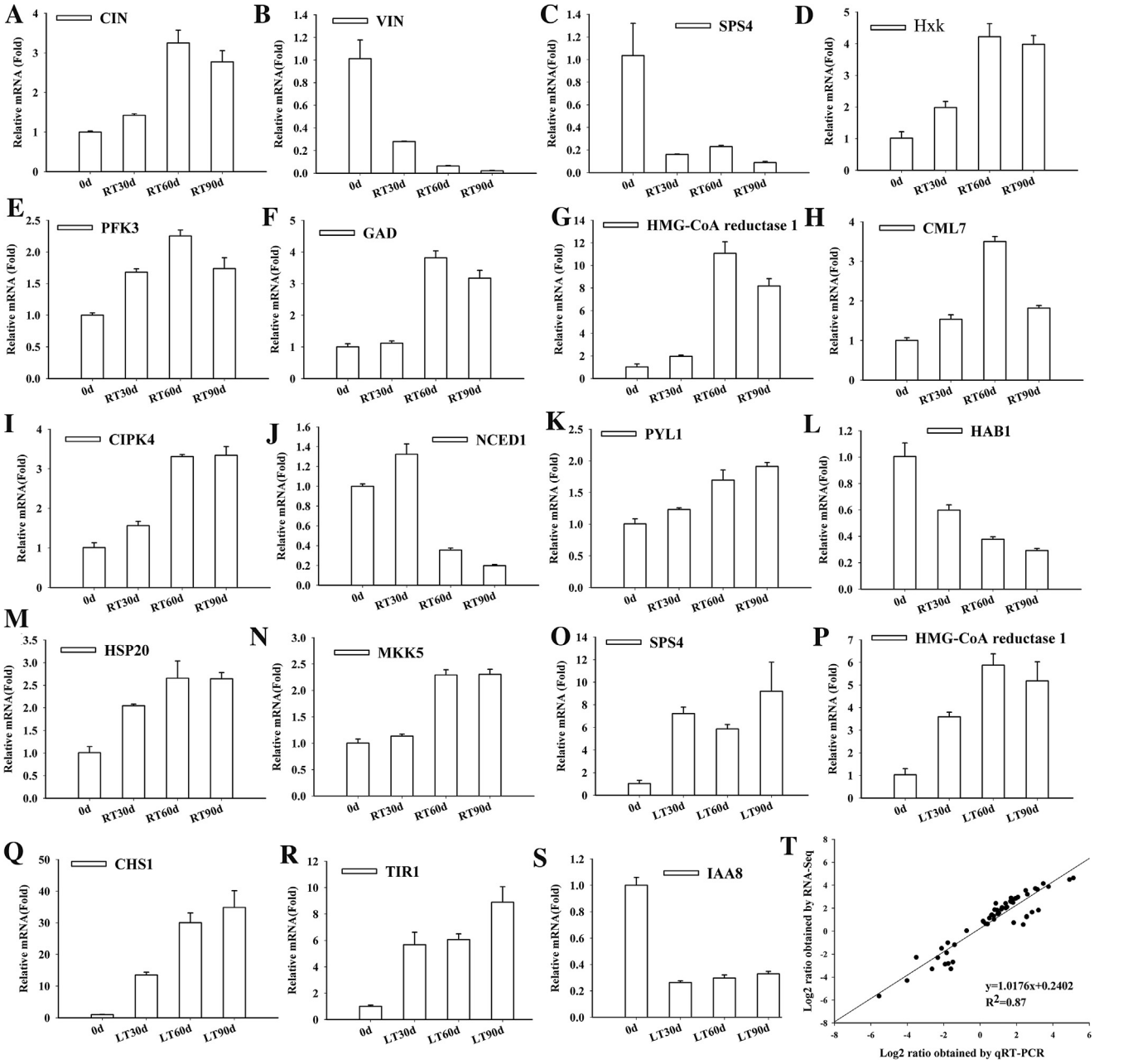

Fig. 3. RNA-Seq validation by quantitative real-time PCR.
Expressions of 17 selected genes associated with sugar metabolism (A) *CIN*, (B)*VIN*, (C) and (O) *SPS4*, (D) *Hxk*, (E) *PFK3*, citrate catabolism (F) *GAD*, (G) and (P) *HMG-CoA reductase 1*, (Q) *CHS1*, signaling (H) *CML7*, (I) *CIPK4*, (N)*MKK5*, hormone biosynthesis and signal transduction (J)*NCED*, (K)*PYL1*, (L)*HAB1*, (R)*TIR1*, (S)*IAA8*, transcription factors (M) *HSP20* were analyzed by qRT-PCR. (A–N) Expression patterns of genes at 30, 60 and 90 days after harvest under room temperature (RT). (O–S) Expression patterns of genes at 30, 60 and 90 days after harvest under low temperature (LT). Relative expression levels were determined based on the reference 0d (control) set to 1. Error bars represent means ± SE ($n = 3$). (T) Correlation between the RNA-Seq data and the qPCR results were revealed by regression analysis using Sigma plot 12.5 software.

3.3. Functional enrichment analysis of DEGs during postharvest storage process

To gain an insight into the biological process of DEGs, MapMan (version3.5.1R2) was employed to draw functional categories. The significantly enriched categories and subcategories were identified ($P < 0.05$), which including hormone metabolism, signaling, glycolysis, secondary metabolism, transport, protein synthesis and degradation, and regulation of transcription factors. These biological pathways under RT and LT storage were differentially regulated (Fig. 4), providing their fundamental roles in fruit senescence.

We found that the majority of DEGs encoding ribosomal proteins (RPLs), considered to be essential for growth and development, exhibited dramatic up-regulation under RT (Supplementary Table S4), which resembles the report that several *RPLs*, such as *RPL11*,were induced in response to salt stress (Omidbakhshfard et al., 2012). These results reflect the increase of large-scale de novo protein synthesis when protein degradation accelerated via up-regulation of ubiquitin (Fig. 4, Supplementary Table S4) during fruit senescence. Previous studies showed that *RPLs* were down-regulated at temperatures below 10 °C in yeast (Hofmann et al., 2012). In our study, *RPLs* were suppressed under LT storage (Supplementary Table S4), illustrating the great roles of RPLs in cold shock response.

Supplementary material related to this article found, in the online version, at http://dx.doi.org/10.1016/j.postharvbio.2015.10.008.

Pathway enrichment analysis showed that DGEs related to transcription factors (TFs) including WRKY, AP2/EREBF, NAC, C2C2-GATA, MYB, AUX/IAA, bHLH, and HB were over-represented (Fig. 4). It is noteworthy that WRKY and NAC transcription factors, known to be crucial for senescence, were induced during leaf senescence processes in Arabidopsis (Breeze et al., 2011) and during short-term storage in orange in response to 2,4-D treatment (Ma et al., 2014). In our results, the majority of identified WRKY and NAC TFs, such as *WRKY33*, *WRKY29*, *WRKY75*, *WRKY22*, *WRKY50*, *WRKY65*, *WRKY19*, *NAC2*, *NAC74*, *NAC100*, *NAC78*, *NAC90*, etc., showed up-

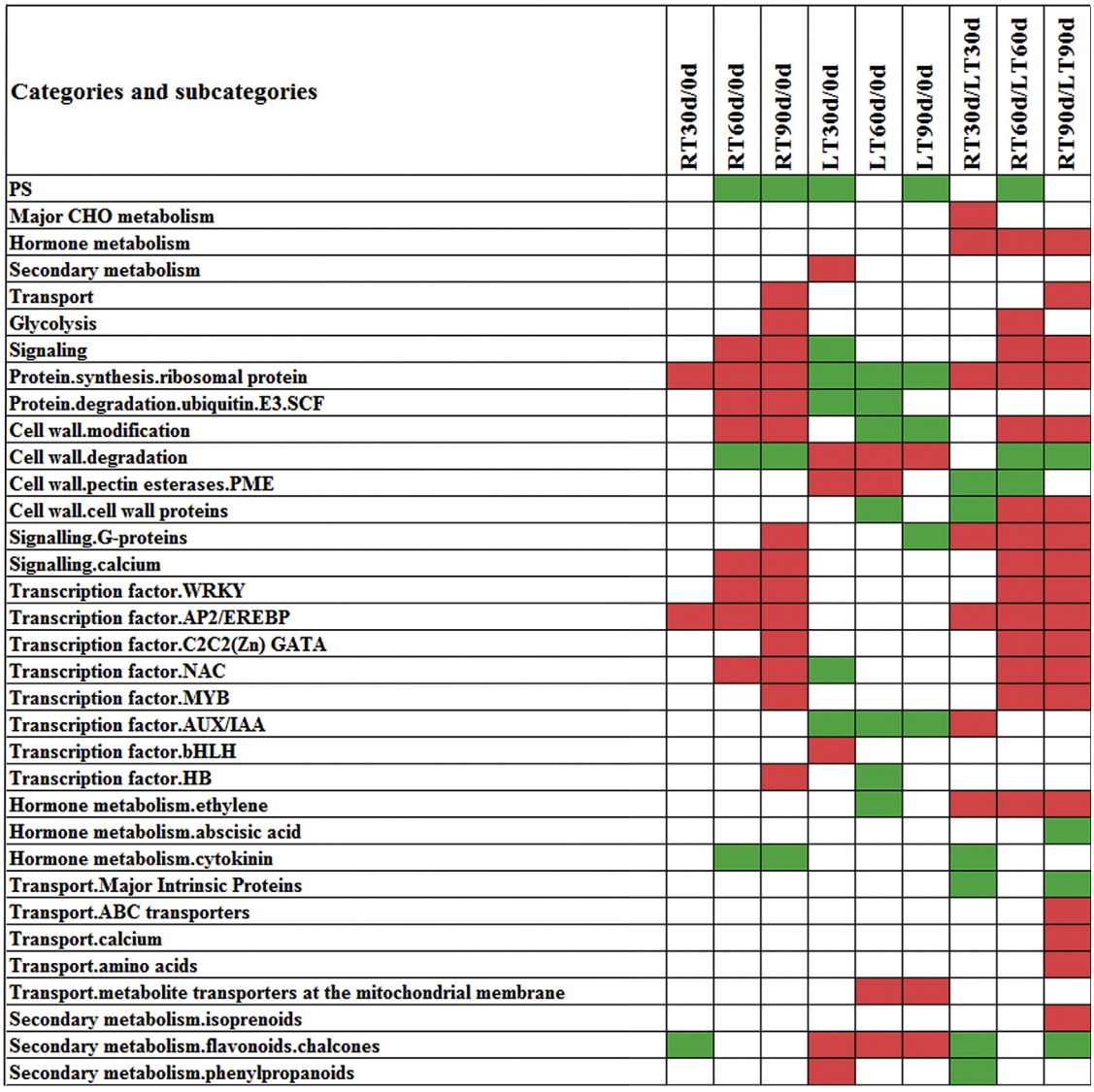

Fig. 4. Functional enrichment analysis of DEGs during postharvest storage process. (For interpretation of the references to color in this figure legend, the reader is referred to the web version of this article.)
The up- and down-regulated DEGs were respectively subjected to MapMan software, and the significantly overrepresented ($P < 0.05$) categories and subcategories at different periods under RT and LT storage were listed. The graph also showed the enriched pathways at each time point under RT storage compared with those under LT storage. Red and green colors indicate the over-represented up- and down-regulated biological pathways, respectively.

regulation at the later stage of RT storage, but down-regulation or no changes under LT (Supplementary Table S4), illustrating that these TFs positively regulate fruit senescence in Powell. However, a previous study suggested that AP2/EREBP and NAC family TFs were mainly present in the loose-skin citrus while tight-skin citrus contains many WRKY (Ding et al., 2015). This indicates that there is a discrepancy between Powell and other tight-skin citrus varieties. In addition, WRKY protein functions through interactions with a series of protein partners, including MAP kinases and CaM, such as MEKK1 (Rushton et al., 2010). Long-term RT storage strongly activated the expression of genes associated with MAP Kinase signaling including *MEKK1*, *MPK20*, *MKK5*, *MEKK2* and *MEKK19* (Supplementary Table S4), indicating that fruit senescence might be promoted by MEKK-WRKY cascades.

3.4. Primary metabolism in Powell fruits was significantly altered during postharvest senescence

In the present study, several DEGs involved in primary metabolism were identified during postharvest senescence (Supplementary Table S5, Fig. 5). We noted that sucrose degradation was followed by accumulation of fructose and glucose under RT (Table 1). It has been reported that sucrose cleavage is mainly mediated by cell wall invertase (CWIN) and acid invertase (VIN) at the early stage of fruit development and by sucrose synthase (SUS) during the later stage of maturation (Katz et al., 2007; Koch, 2004; Liu et al., 2013). *Neutral/alkaline invertase* (*CIN*) were also reported to be increased in the expressions towards fruit maturation (Lin et al., 2015). In this study, *SUS1* and *CINs* were up-regulated under

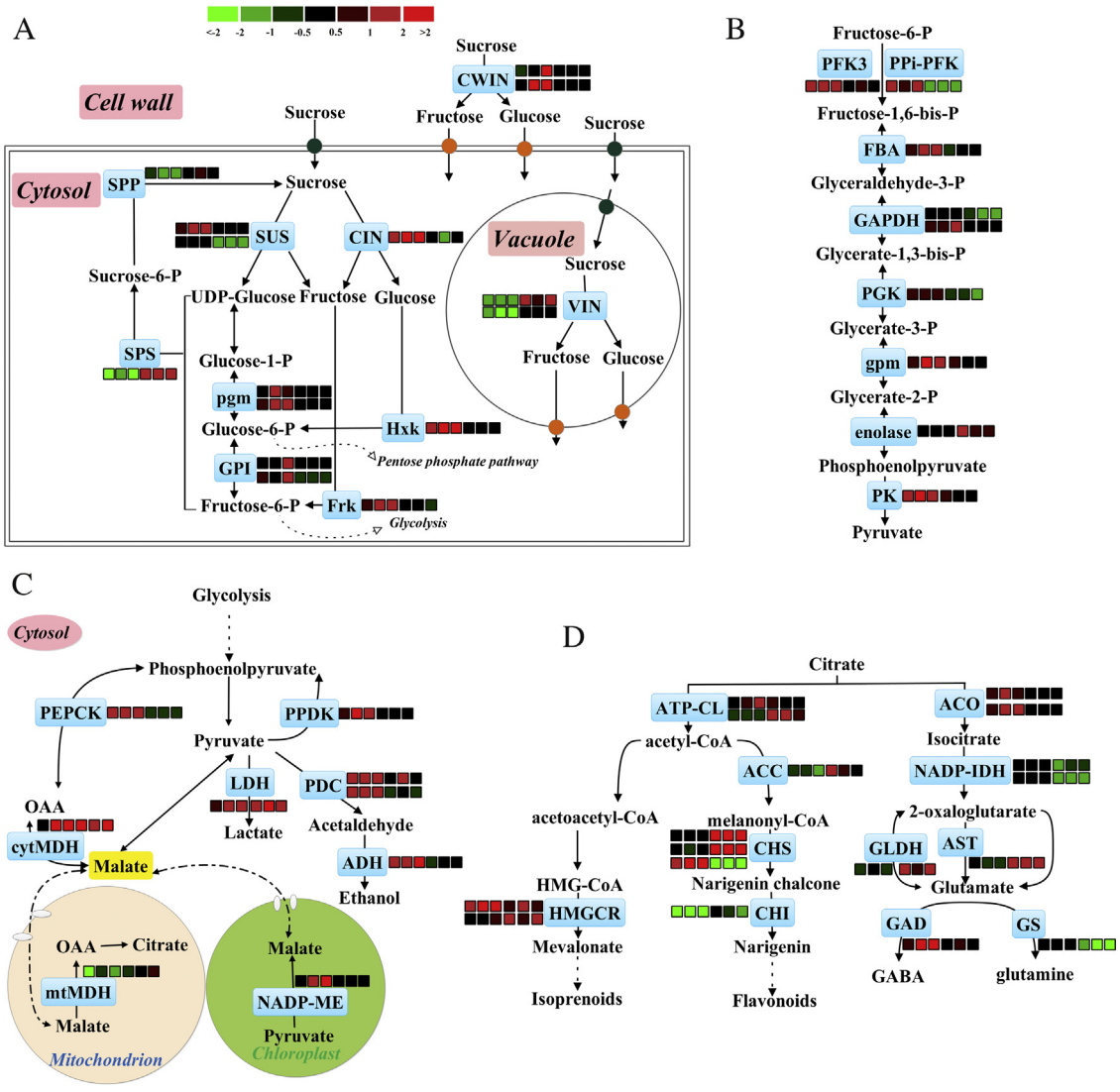

Fig. 5. Transcriptomic mapping of genes associated with primary metabolism during postharvest storage of Powell fruits. (For interpretation of the references to color in this figure legend, the reader is referred to the web version of this article.)
Metabolic pathways related to sucrose degradation (A), glycolysis (B), malate degradation (C) and citrate metabolism (D) during postharvest storage in Powell fruits were mapped. Expression profile for each gene was shown in colored blocks. The first 3 squares represent mRNA levels at 30, 60 and 90 days under RT, and the following squares represent mRNA levels under LT compared to control (from left to right). The expression changes were represented by log2 ratio. Red colors/green colors correspond to up-/down-regulation of these genes, and $\log_2$ ratio ≥ 1 is considered statistically significant. Details were showed in Supplementary Table S5. CWIN, cell wall invertase; CIN, neutral/alkaline invertase; VIN, vacuole invertase; Hxk, hexokinase; Frk, fructokinase; SUS, sucrose synthase; SPS, sucrose phosphate synthase; SPP, sucrose phosphatase; pgm, phosphoglucomutase; GPI, glucose-6-phosphate isomerase; PFK3, 6-phosphofructokinase 3; PPi-PFK, pyrophosphate-dependent phosphofructokinase; FBA, fructose-bisphosphate aldolase; GAPDH, glyceraldehyde-3-phosphate dehydrogenase; PGK, phosphoglycerate kinase; gpm, phosphoglycerate mutase; PK, pyruvate kinase; MDH, malate dehydrogenase; NADP-ME, NADP-dependent malic enzyme; PEPCK, PEP carboxykinase; PPDK, pyruvate orthophosphate dikinase; PDC, pyruvate decarboxylase; LDH, lactate dehydrogenase; ADH, alcohol dehydrogenase; ACO, aconitase; NADP-IDH, NADP-dependent isocitrate dehydrogenase; GLDH, glutamate dehydrogenase; AST, aspartate aminotransferase;GAD, glutamate decarboxylase; GS, glutamine synthetase; ATP-CL, ATP-citrate lyase; ACC, acetylcoenzyme A carboxylase; HMGCR, hydroxy methylglutaryl CoA reductase; CHS, chalcone synthase; CHI, chalcone-flavonone isomerase

RT storage (Fig. 5A), indicating that both routes of sucrose degradation are activated during fruit senescence. Down-regulation of *VINs* and *sucrose phosphate synthase 4* (*SPS4*) under RT storage (Fig. 5A) may increase the concentration gradients leading to sucrose partitioning in favor of cytoplasm (Ayre, 2011), thus adequate glucose and fructose were derived for glycolysis and ATP production. Ding et al. (2015) demonstrated that sugar transporters are pivotal affecting senescence process in citrus, such as sucrose transporter 1 (SUT1). In the present study, a *SUT3* gene (Cs7g04100) was increased in its mRNA level under long-term RT storage, but flat under LT (Supplementary Table S3), suggesting that sucrose exporting may contribute to sucrose degradation in Powell fruits during postharvest senescence. Up-regulation of *hexokinase* (*Hxk*) and *fructokinase* (*Frk*) (Fig. 5A), were also observed during leaf senescence (Dai et al., 1999) and fruit ripening (Lin et al., 2015), indicating their potential roles in fruit senescence. Besides, these sugars also exert signaling roles via cross-talk with hormone and ROS (Liu et al., 2013). Hence, sucrose degradation under RT storage could be vital, which results in accumulation of hexoses (Table 1) and consequently induces fruit senescence (Wingler and Roitsch, 2008) during postharvest period. Accordingly, no remarkable changes in concentration of sugars were found during LT storage (Supplementary Table S2). This was in accordance with the observation that the genes associated with sugar metabolism remained largely unchanged under LT (Fig. 5A), which would lead to catabolism inhibition and delayed fruit senescence.

Supplementary material related to this article found, in the online version, at http://dx.doi.org/10.1016/j.postharvbio.2015.10.008.

RNA-Seq showed that the overwhelming majority of DEGs were transcriptionally induced under RT including *phosphofructokinase* (*PFK*), *pyrophosphate-dependent 6-phosphofructokinase* (*PPi-PFK*), *fructose-bisphosphate aldolase* (*FBA*), *glyceraldehyde-3-phosphate-dehydrogrnase* (*GAPDH*), *phospho-glycerate mutase* (*gpmA*) and *pyruvate kinase* (*PK*) (Fig. 5B). The acceleration of glycolysis pathway indicates a faster carbon flow through the glycolysis pathway under RT storage. In contrast to RT storage, the transcripts of enzymes associated with glycolysis are maintained or even decreased under LT storage (Fig. 5B), and therefore fruit senescence might be delayed. This resembles earlier result of Jiang et al. (2014) that heat and 1-MCP treatment effectively postponed postharvest ripening via inhibiting glycolysis in peach.

Fruits stored at RT underwent loss of malate (Table 1). A recent study showed that there were correlations between malate and malic dehydrogenase (MDH) (Ding et al., 2015). However, up-regulation of *cytMDH* and the opposite expression pattern of *mMDH* were observed (Fig. 5C), indicates that MDH may not facilitate malate degradation during RT storage. Malate may be converted to PEP via oxaloacetate or pyruvate, through PEP carboxykinase (PEPCK) or pyruvate orthophosphate dikinase (PPDK). RNA-Seq showed that *PEPCK* and *PPDK* were up-regulated under RT (Fig. 5C), suggesting its contribution to malate degradation. This resembles previous reports that the increase of *PEPCK* in expression coincided with the malate loss during fruit ripening in grape (Sweetman et al., 2009), raspberry, blueberry and red currant (Famiani et al., 2005). As yet, similar results demonstrated that higher temperature storage elevated the abundance of PPDK protein along with decreased malate concentration in peach fruit (Lara et al., 2009). Thus, our result shares the viewpoint that the utilization of malate is favored in gluconeogenesis during fruit senescence. The released malate could be functioned through involvement in fermentation pathway during fruit ripening (Sweetman et al., 2009) and storage

Table 2
DEGs associated with calcium signaling during postharvest storage in Powell fruit.

Accession no.	Log 2 ratio (samples/0d)						Gene annotation
	RT30d	RT60d	RT90d	LT30d	LT60d	LT90d	
Calcium-binding protein, CML							
Cs1g23590	–	–	–	–	−2.24	−3.46	CML41
Cs4g05510	1.407	2.5	2.43	–	–	–	CML7
Cs4g11690	–	2.57	2.24	–	−1.72	−1.82	CMLPBP1
Cs5g07160	1.533	5.27	4.97	–	–	–	CML19
Cs5g22810	–	2.46	1.87	–	–	–	CML3
Cs6g10520	3.049	6.37	5.81	–	–	−1.65	CML43
Cs6g17590	2.913	6.99	6.57	–	–	–	CML23
Cs6g21420	1.434	4.9	4.73	1.06	–	–	CML45
Cs9g11850	–	1.2	1.51	–	–	–	CML29
orange1.1t00071	2.93	4.8	4.06	–	–	–	CML27
orange1.1t00531	1.064	1.13	1.06	2.123	–	1.478	CMLKIC
orange1.1t04034	1.532	3.44	3.21	–	1.414	–	CML37
Calcineurin B-like protein, CBL							
Cs1g18400	–	−1.6	−1.3	–	–	–	CBL9
Cs4g18590	–	–	−1.1	–	–	–	CBL10
CBL-interacting protein kinase, CIPK							
Cs2g04710	–	1.45	1.53	–	–	–	CIPK12
Cs2g09400	1.135	1.18	1.88	–	–	–	CIPK11
Cs6g09730	–	1.79	1.94	–	–	–	CIPK2
Cs6g09770	–	–	–	−1.32	−1.77	−1.62	CIPK14
Cs9g01260	–	1.32	1.3	1.256	–	1.473	CIPK1
Cs9g08000	1.431	2.56	2.63	−1.73	−1.18	−1.39	CIPK4
orange1.1t02758	–	−1.4	−1.3	−1.43	−1.28	−1.6	CIPK25
Calcium-dependent protein kinase, CPK							
Cs4g10330	–	1.5	1.47	–	–	–	CPK9
Cs5g04380	–	–	1.05	–	–	–	CPK30
Cs8g01240	–	1.86	1.5	–	–	–	CPK4
Cs9g12450	–	2.16	1.67	–	–	1.049	CPK32
Cs9g16760	–	–	–	−1.07	–	−1.05	CPK17

(Tietel et al., 2011). The mRNA levels of *pyruvate decarboxylase* (*PDC*) and *alcohol dehydrogenase1* (*ADH1*) were strongly up-regulated under RT (Fig. 5C), suggesting a link between malate degradation and fermentative metabolism (Selvaraj, 1993). It was supported by the evidence that the volatiles such as ethanol and acetaldehyde showed an increase from 30 DAH to 90 DAH under RT storage (Supplementary Fig. S1). Taken together, malate was utilized as carbon source for energy supply during high rates of fruit metabolism. Accordingly, no remarkable changes were found in malate content and malate metabolism related genes during LT storage (Supplementary Table S2, Fig. 5C).

Supplementary material related to this article found, in the online version, at http://dx.doi.org/10.1016/j.postharvbio.2015.10.008.

In this work, two *aconitate hydratase 3* (*ACO3*) and a *glutamate decarboxylase* (*GAD*, orange1.1t01622) were identified to be increased in their transcripts under RT storage (Fig. 5D). The result suggested that the loss of citric acid was predictively attributed to activation of GABA shunt pathway (Cercos et al., 2006), which has been supported by the accumulation of GABA during the later stage of RT storage (Table 1). Besides, there might be a correlation between citrate catabolism and acetyl-CoA metabolism (Katz et al., 2007). Up-regulation of *ATP-citrate lyase* (*ATP-CL*) and *HMG-CoA reductase* (*HMGCR*) (Fig. 5D), indicates that acetyl-CoA metabolism was also activated under RT storage, which is consistent with the concept in "Ponkan" during fruit maturation (Lin et al., 2015). By contrast, several genes related to these two pathways including *NADP-IDH*, *glutamine synthetase* (*GS*), *aspartate aminotransferase* (*AST*), *glutamate dehydrogenase* (*GLDH*), *ATP-CL*, *HMGCR* and *chalcone synthase* (*CHS*) showed differential expression patterns during LT storage (Fig. 5D). These results herein demonstrated that citrate catabolism differed between RT and LT storage.

Table 3
DEGs associated with hormone metabolism and signaling during Powell fruit storage.

Accession no.	Log2 ratio (samples/0d)						Gene Annotation
	RT30d	RT60d	RT90d	LT30d	LT60d	LT90d	
ABA biosynthesis and signaling							
Cs5g14370	–	−2.89	−2.09	1.444	–	–	NCED3
Cs2g03270	–	−2.69	−2.31	–	–	–	NCED2
Cs7g14820	–	−2.53	−1.43	–	–	–	NCED4
Cs8g14150	−3	−3	−Inf	–	–	–	NCED4
Cs8g05940	2.199	1.563	2.032	−3.81	−1.49	−3.81	ABA 8ox4
Cs8g13770	–	–	−1.87	1.375	1.196	1.171	AAO3
Cs4g18640	–	Inf	Inf	Inf	–	Inf	PYL2
orange1.1t01026	–	1.034	1.837	–	–	–	PYL1
Cs4g05690	–	−1.18	−1	–	–	–	HAB1
Cs4g15360	–	−1.67	−1.09	–	–	–	AHG3/PP2CA
Cs4g01010	–	1.766	1.592	–	–	–	PP2C 9
Cs8g20420	2.19	6.501	5.961	–	–	–	PP2C 2
Cs3g21410	1.045	1.742	1.247	–	–	–	ABI5-like
Ethylene perception and signaling							
Cs1g21210	−2.147	–	−1.954	−1.7	−3.7	−Inf	ACS8
orange1.1t00416	–	2.939	2.322	3.931	3.044	2.248	ACS2
Cs2g20590	–	–	–	–	–	1.379	ACO
Cs9g09030	–	–	−1.317	–	–	–	ACO homolog 1
Cs9g09040	–	−1.052	–	–	–	–	ACO homolog 6
Cs9g09050	–	–	−1.495	−1.379	−1.198	−1.115	ACO homolog 1
Cs8g12880	–	−1.15	−1.22	–	–	–	ERS3
Cs9g08850	1.632	2.397	2.105	–	–	–	ERS2
Cs3g06950	–	–	1.167	–	–	–	EIN3
Cs7g05390	–	1.157	1.214	–	–	–	EBF1
Cs4g17960	–	2.003	2.229	–	–	–	EBF
Cs1g01320	–	−1.75	−1.02	–	−1.09	−1.28	ERF060
Cs1g07950	–	3.516	3.163	–	–	–	ERF4
Cs2g20500	–	2.301	2.132	–	–	–	ERF3/PTI6
Cs3g18470	–	–	1.019	–	–	–	RAP2-4
Cs4g09770	1.205	3.273	2.908	–	–	−1.16	ERF7
Cs5g10240	4.087	8.285	7.931	–	–	–	CBF/DREB
Cs5g33540	–	1.358	1.843	−1.38	–	–	RAP2-3/PTI5
Cs2g05280	–	2.011	2.69	−1.79	−3.38	−3.38	ERF1
Cs3g21660	–	–	1.568	–	1.076	1.749	ERF110
Auxin perception, transport and signaling							
Cs2g06880	–	–	–	3.55	3.215	3.636	TIR1
Cs6g07990	–	−1.4	−2.54	–	–	–	AUX2/LAX
Cs7g31320	−1.49	−2.13	−3.38	–	–	–	AUX1/LAX
Cs2g09440	–	−1.07	−1.78	–	–	–	ARF6
Cs6g16030	–	–	−1.17	–	–	–	ARF8
Cs4g16220	−Inf	−2.25	−1.93	–	–	1.585	IAA27
Cs1g15390	–	–	–	−2.88	−2.82	−3.29	IAA8
Cs3g16750	–	–	–	−1.61	−1.67	−1.75	IAA9
Cs9g09120	–	–	−1.1	−2.55	−2.99	−3.09	IAA13
Cs1g13960	1.227	0.405	0.504	−1.57	−2.56	−3.8	IAA14
Cs4g18240	1.459	5.426	5.304	−1	−1.59	−Inf	IAA29
Cs4g04520	–	–	–	−2.06	−2.16	−2.22	ARF5

3.5. The potential role of calcium signaling on fruit senescence

The processes of fruit ripening and senescence are generally regulated by calcium signals (Aghdam et al., 2012), which is provided by the direct evidence that overexpression of a H^+/Ca^{2+} transporter (*CAX4*) in tomatoes elevated fruit Ca^{2+} level and prolonged shelf life (Park et al., 2005). Calcium signals can be perceived by sensor proteins including calcium binding proteins (CaBPs) /calmodulin-like proteins (CMLs), calcineurin B-like protein (CBLs) and calcium-dependent protein kinase (CPKs), thus modulating down-stream reactions (Yu et al., 2014). In the present study, 27 genes associated with calcium signaling were observed to be prominently regulated. Of them, the vast majority showed remarkable up-regulation under RT, and exhibited flat or decreases in their expressions during LT storage correspondingly (Table 2). In plants, CMLs function in the processes including development, abiotic stress responses and hormone signaling (Bender and Snedden, 2013). Few reports focused on the role of CMLs in fruit. Very recently, Zhang et al. (2011, 2012) showed that the abundance of CaBPs were elevated by heat and ethephone treatments, but suppressed by 1-MCP treatment during postharvest fruit ripening in peach. CaBPs might be involved in the regulation of HSPs, therefore enhance self-defense in response to ROS produced by fruit senescence (Jiang et al., 2014) or activate the hormones/systemic signals such as salicylic acid (SA), cytokinin and jasmonic acid (JA) to regulate fruit ripening (Manjunatha et al., 2010). Here, we found that during the later stages of RT storage, the overwhelming majority of *CMLs* (11/12, such as *CML3*, *CML7*, *CML19*, *CML23*, *CML27*, *CML29*, *CML43*, *CML45*, *CMLPBP1*) and *HSPs* were strongly induced (Table 2, Supplementary Table S4), suggesting their involvement in fruit senescence. It is reported that several CBL-interacting protein kinase (CIPKs) including *CIPK1* and *CIPK11* were positively regulated by various abiotic stresses such as ABA, drought and salt (Yu et al., 2014). Also, CIPK and CDPK were observed to be significantly changed in abundance during mature-fruit abscission in melon, indicating a possible critical role of these kinases in senescence (Corbacho et al., 2013). In our study, the majority members of *CIPKs* (5/7, including *CIPK1*, *CIPK2*, *CIPK4*, *CIPK11* and *CIPK12*) and *CPKs* (4/5, including *CPK4*, *CPK 9*, *CPK 30* and *CPK 32*) showed significant up-regulation during long-term RT storage (Table 2). Given that CBL–CIPKs and CDPKs are involved in ABA signaling pathway (Yu et al., 2014; Zhang, 2014), and CDPKs play a prominent role in tomato ethylene signal transduction via phosphorylating ACS, a key enzyme for ethylene synthesis (Sebastià et al., 2004), we hypothesized that the regulation of CIPKs and CDPKs in fruit senescence may be mediated by ABA and ethylene signaling cascades during postharvest storage in citrus.

3.6. Fruit senescence was regulated by ABA, ethylene and auxin during storage

In the present study, several genes involved in hormone metabolism and signaling were dramatically altered during postharvest senescence and showed discrepant expression patterns between RT and LT storage (Table 3). ABA plays a fundamentally important role in induction and maintenance of fruit ripening and senescence (Cara and Giovannoni, 2008; Leng et al., 2014). A previous study has provided the evidence that decrease of ABA levels by suppressing *NCED1* in tomato led to down-regulation of the genes related to cell wall degradation, such as *PG*, *PME* and *XET*, which favored a significant extension of the shelf life (Sun et al., 2012). Our results showed that *NCEDs* including *NCED2*, *NCED3*, *NCED4* (Cs7g14820) and *NCED4* (Cs8g14150), key genes involved in ABA synthesis, were down-regulated during long-term RT storage (Table 3), indicating a correlation between ABA and *Powell* fruit senescence. It was partially consistent with the results reported by Ding et al. (2015) that decreased expression of *NCED4* was observed during fruit senescence in citrus species. Yun et al. (2012) found that low temperature storage delayed fruit senescence by decreasing ABA content. However, there was no remarkable difference in *NCEDs* expression profiles observed under LT in our data (Table 3). Subsequently, ABA signal transduction modulates ABA response via "PYR/PYLs-PP2Cs-SnRK2s-AREB/ABFs" pathway, and then facilitates the process of fruit ripening. It is worth noting that ABA signal was enhanced by the up-regulation of *PYLs* and *ABI5* and the down-regulation of *HAB* and *AHG3* during the later stage of RT storage. Accordingly, no obvious changes were found in ABA signaling pathway under LT storage (Table 3). Previous reports suggested that down-regulation of *PYR1* and *ABI1* could inhibit and promote fruit ripening in strawberry, respectively (Chai et al., 2011; Jia et al., 2013). In tomato, *AREB1*-overexpressing lines led to hexose accumulation via up-regulation of *VIN* and *SUS*, thus affecting fruit development (Bastías et al., 2014). On the basis of these results, ABA metabolism and signaling might be a characteristic feature present in citrus fruit during long-term storage (Yun et al., 2012). Although ABA biosynthesis probably decrease, the enhanced ABA response by *PYL1/PYL2-ABI5* cascades could promote the expression of genes related to sugar metabolism (Fig. 5A), cell wall degradation including *PG*, *PME*, *XET* and *Exp*, and ROS such as *RBOH* (Supplementary Table S3), finally accelerating fruit senescence.

Increasing evidence has indicated that ethylene is involved in regulation of maturation and senescence in non-climacteric citrus fruit. As reported by Goldschmidt (1997), exogenous ethylene led to the induction of ripening in citrus fruit peel. A study has also revealed that auxin (2,4-D) treatments reversed fruit senescence by inhibiting ethylene production during short-term storage in citrus (Ma et al., 2014). Our data showed that some DEGs associated with ethylene synthesis were down-regulated such as ACS8 and ACO homolog1, and also exhibited same expression profiles under RT and LT storage (Table 3), suggesting that ethylene synthesis pathway may not be involved in fruit senescence in Powell. Interestingly, Ludwig et al. (2005) reported that elevated CDPK signaling mediated inhibition of stress-induced MAPK activation through enhancing ethylene production in response to biotic/abiotic stress. In our results, CDPK and MAPK transcripts were both up-regulated during RT- induced fruit senescence (Table 2, Supplementary Table S4), which might be attributed to the tiny change of ethylene synthesis. It is distinguished from the reports that some ACOs and ACSs were up-regulated during citrus senescence (Ding et al., 2015), indicating that there is different in ethylene-mediated senescence between citrus varieties. In addition, genes involved in ethylene perception and signal transduction were significantly regulated during RT storage (Table 3). Especially, the majority of *ERFs* (7 out of 9) including *ERF4*, *ERF3/PTI6*, *RAP2-4*, *ERF7*, *CBF/DREB*, *RAP2-3/PTI5* and *ERF1* displayed dramatic up-regulation under RT storage and differed between RT and LT, indicating that the increase in ethylene response could promote the process of fruit senescence during postharvest storage.

It has been reported that auxin plays a vital role in the suppression of abscission and senescence. In the present study, several genes participating in auxin transport and signaling were dramatically modulated, indicating the involvement of these DEGs in fruit senescence. During long-term RT storage, *AUX1* and *AUX2* displayed down-regulation (Table 3), which could result in a reduced auxin import and induction of fruit senescence. Interestingly, *PaLAX1*-overexpression lines, with excessive levels of free endogenous auxin, exhibited chlorotic phenotype in mature leaves and accelerated senescence (Hoyerová et al., 2008). These results appear to indicate that senescence might be promoted when auxin homeostasis is altered. In addition, senescence regulated by auxin is initiated and/or mediated through auxin signaling cascades including TIR1, Aux/IAAs and ARFs. A recent study found that

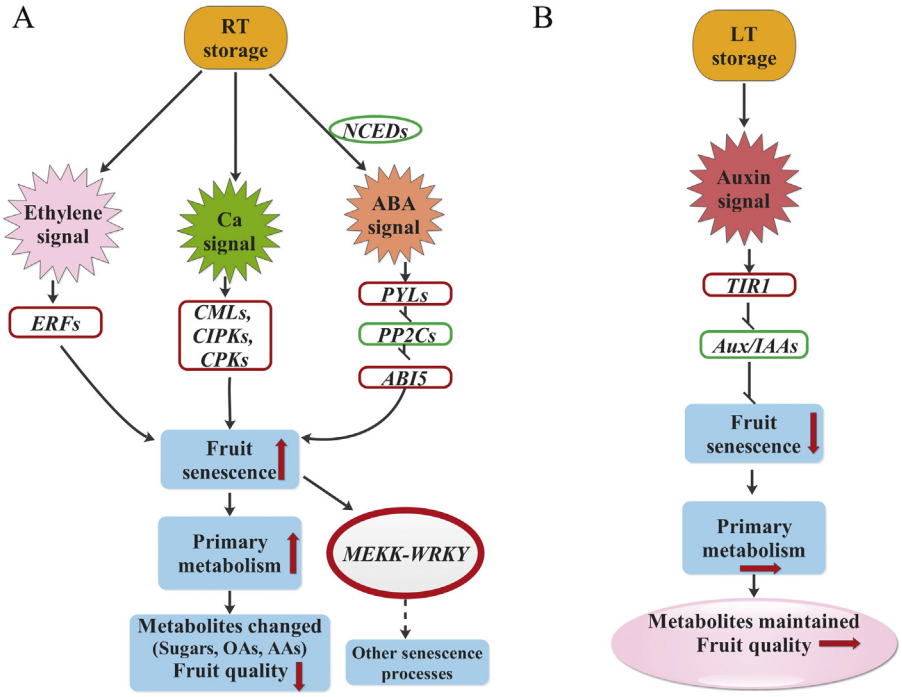

Fig. 6. A working hypothesis of metabolic and regulatory pathway during fruit senescence. (For interpretation of the references to color in this figure legend, the reader is referred to the web version of this article.)
(A) RT storage increases the response of calcium, ABA and ethylene signals via up-regulation of genes including *CMLs*,*CIPKs*, *CPKs*, *PYLs*, *ABI5-like* and *ERFs*, which could positively regulate fruit senescence. Subsequently, primary metabolism was induced and resulted in the declines of metabolites such as sucrose and organic acids and finally the loss of fruit quality. (B) LT storage might accelerate the auxin signal, which could inhibit senescence, and therefore maintaining the levels of metabolites and fruit quality. The red and green frame showed up- and down-regulation of genes, respectively. Dashed line shows suggested interactions.

ARF2 is involved in regulation of leaf senescence, from the evidence that *arf2* mutants exhibited delays in several processes related to plant aging (Ellis et al., 2005). Our data showed that the transcripts of *ARF6* and *ARF8*, activators of auxin signaling (Guilfoyle and Hagen, 2007), were inhibited during long-term RT storage (Table 3), which could reduce auxin sensitivity, thus accelerating fruit senescence. This result is consistent with the study in lily that *ARF6/8* was found to be down-regulated during tepal senescence (Lombardi et al., 2015). During LT storage, *TIR1*, a positive regulator, was observed to be significantly up-regulated, and some *Aux/IAAs* including *IAA8*, *IAA9*, *IAA13*, *IAA14* and *IAA29*, repressors of auxin signaling, were remarkably suppressed (Table 3), which might accelerate the auxin signal and then inhibit senescence.

4. Conclusion

In conclusion, a hypothesis of metabolic and regulatory pathway during fruit senescence was presented (Fig. 6). RT storage increases the response of calcium, ABA and ethylene signals via up-regulation of genes associated with signaling transduction including *CMLs*, *CIPKs*, *CPKs*, *PYLs*, *ABI5-like* and *ERFs*, which could positively regulate fruit senescence. Subsequently, primary metabolism was induced and resulted in the declines of metabolites such as sucrose and organic acids and finally the loss of fruit quality. Accordingly, LT storage might accelerate the auxin signal, which could inhibit senescence, and therefore maintaining the levels of metabolites and fruit quality.

Acknowledgements

This work was supported by grants from the National High Technology Research and Development Program of China (2012AA101702), the National Basic Research Program of China (2013CB127106, 2013CB127101), and Fundamental Research Funds for the Central Universities (CDJXS11232245).

References

Aghdam, M.S., Hassanpouraghdam, M.B., Paliyath, G., Farmani, B., 2012. The language of calcium in postharvest life of fruits, vegetables and flowers. Sci. Hortic. 144, 102–115.
Ayre, B.G., 2011. Membrane-transport systems for sucrose in relation to whole-plant carbon partitioning. Mol. Plant ssr014.
Bastías, A., Yañez, M., Osorio, S., Arbona, V., Gómez-Cadenas, A., Fernie, A.R., Casaretto, J.A., 2014. The transcription factor AREB1 regulates primary metabolic pathways in tomato fruits. J. Exp. Bot. eru114.
Bender, K.W., Snedden, W.A., 2013. Calmodulin-related proteins step out from the shadow of their namesake. Plant Physiol. 163, 486–495.
Breeze, E., Harrison, E., McHattie, S., Hughes, L., Hickman, R., Hill, C., Kiddle, S., Kim, Y.-s., Penfold, C.A., Jenkins, D., 2011. High-resolution temporal profiling of transcripts during *Arabidopsis* leaf senescence reveals a distinct chronology of processes and regulation. Plant Cell Online 23, 873–894.
Buchanan-Wollaston, V., 1997. The molecular biology of leaf senescence. J. Exp. Bot. 48, 181–199.
Cara, B., Giovannoni, J.J., 2008. Molecular biology of ethylene during tomato fruit development and maturation. Plant Sci. 175, 106–113.
Cercos, M., Soler, G., Iglesias, D.J., Gadea, J., Forment, J., Talon, M., 2006. Global analysis of gene expression during development and ripening of citrus fruit flesh. A proposed mechanism for citric acid utilization. Plant Mol. Biol. 62, 513–527.
Cerdán-Calero, M., Sendra, J.M., Sentandreu, E., 2012. Gas chromatography coupled to mass spectrometry analysis of volatiles, sugars, organic acids and aminoacids in valencia late orange juice and reliability of the automated mass spectral deconvolution and identification system for their automatic identification and quantification. J. Chromatogr. A 1241, 84–95.
Chai, Y.-m., Jia, H.-f., Li, C.-l., Dong, Q.-h., Shen, Y.-y., 2011. FaPYR1 is involved in strawberry fruit ripening. J. Exp. Bot. 62, 5079–5089.
Chen, M., Jiang, Q., Yin, X.-R., Lin, Q., Chen, J.-Y., Allan, A.C., Xu, C.-J., Chen, K.-S., 2012. Effect of hot air treatment on organic acid- and sugar-metabolism in Ponkan (*Citrus reticulata*) fruit. Sci. Hortic. 147, 118–125.
Corbacho, J., Romojaro, F., Pech, J.-C., Latché, A., Gomez-Jimenez, M.C., 2013. Transcriptomic events involved in melon mature-fruit abscission comprise the sequential induction of cell-wall degrading genes coupled to a stimulation of endo and exocytosis. PLoS One 8, e58363.
Dai, N., Schaffer, A., Petreikov, M., Shahak, Y., Giller, Y., Ratner, K., Levine, A., Granot, D., 1999. Overexpression of Arabidopsis hexokinase in tomato plants inhibits

growth, reduces photosynthesis, and induces rapid senescence. Plant Cell Online 11, 1253–1266.
Ding, Y., Chang, J., Ma, Q., Chen, L., Liu, S., Jin, S., Han, J., Xu, R., Zhu, A., Guo, J., Luo, Y., Xu, J., Xu, Q., Zeng, Y., Deng, X., Cheng, Y., 2015. Network analysis of postharvest senescence process in citrus fruits revealed by transcriptomic and metabolomic profiling. Plant Physiol. 168, 357–376.
Ellis, C.M., Nagpal, P., Young, J.C., Hagen, G., Guilfoyle, T.J., Reed, J.W., 2005. AUXIN RESPONSE FACTOR1 and AUXIN RESPONSE FACTOR2 regulate senescence and floral organ abscission in *Arabidopsis thaliana*. Development 132, 4563–4574.
Famiani, F., Cultrera, N.G., Battistelli, A., Casulli, V., Proietti, P., Standardi, A., Chen, Z.-H., Leegood, R.C., Walker, R.P., 2005. Phosphoenolpyruvate carboxykinase and its potential role in the catabolism of organic acids in the flesh of soft fruit during ripening. J. Exp. Bot. 56, 2959–2969.
Goldschmidt, E.E., 1997. Ripening of citrus and other non-climacteric fruits: a role for ethylene. VIII International Symposium on Plant Bioregulation in Fruit Production 463 335–340.
Guilfoyle, T.J., Hagen, G., 2007. Auxin response factors. Curr. Opin. Plant Biol. 10, 453–460.
Hofmann, S., Cherkasova, V., Bankhead, P., Bukau, B., Stoecklin, G., 2012. Translation suppression promotes stress granule formation and cell survival in response to cold shock. Mol. Biol. Cell 23, 3786–3800.
Hoyerová, K., Perry, L., Hand, P., Laňková, M., Kocábek, T., May, S., Kottová, J., Pačes, J., Napier, R., Zažímalová, E., 2008. Functional characterization of PaLAX1, a putative auxin permease, in heterologous plant systems. Plant Physiol. 146, 1128–1141.
Jia, H.-f., Lu, D., Sun, J.-h., Li, C.-l., Xing, Y., Qin, L., Shen, Y.-y, 2013. Type 2C protein phosphatase ABI1 is a negative regulator of strawberry fruit ripening. J. Exp. Bot. 64, 1677–1687.
Jiang, L., Zhang, L., Shi, Y., Lu, Z., Yu, Z., 2014. Proteomic analysis of peach fruit during ripening upon post-harvest heat combined with 1-MCP treatment. J. Proteom. 98, 31–43.
Katz, E., Fon, M., Lee, Y., Phinney, B., Sadka, A., Blumwald, E., 2007. The citrus fruit proteome: insights into citrus fruit metabolism. Planta 226, 989–1005.
Koch, K., 2004. Sucrose metabolism: regulatory mechanisms and pivotal roles in sugar sensing and plant development. Curr. Opin. Plant Biol. 7, 235–246.
Lara, M.V., Borsani, J., Budde, C.O., Lauxmann, M.A., Lombardo, V.A., Murray, R., Andreo, C.S., Drincovich, M.F., 2009. Biochemical and proteomic analysis of 'Dixiland' peach fruit (*Prunus persica*) upon heat treatment. J. Exp. Bot. erp267.
Leng, P., Yuan, B., Guo, Y., Chen, P., 2014. The role of abscisic acid in fruit ripening and responses to abiotic stress. J. Exp. Bot. eru204.
Lin, Q., Wang, C., Dong, W., Jiang, Q., Wang, D., Li, S., Chen, M., Liu, C., Sun, C., Chen, K., 2015. Transcriptome and metabolome analyses of sugar and organic acid metabolism in Ponkan (*Citrus reticulata*) fruit during fruit maturation. Gene 554, 64–74.
Liu, Y.-H., Offler, C.E., Ruan, Y.-L., 2013. Regulation of fruit and seed response to heat and drought by sugars as nutrients and signals. Front. Plant Sci. 4.
Lombardi, L., Arrom, L., Mariotti, L., Battelli, R., Picciarelli, P., Kille, P., Stead, T., Munné-Bosch, S., Rogers, H.J., 2015. Auxin involvement in tepal senescence and abscission in Lilium: a tale of two lilies. J. Exp. Bot. 66, 945–956.
Ludwig, A.A., Saitoh, H., Felix, G., Freymark, G., Miersch, O., Wasternack, C., Boller, T., Jones, J.D., Romeis, T., 2005. Ethylene-mediated cross-talk between calcium-dependent protein kinase and MAPK signaling controls stress responses in plants. Proc. Natl. Acad. Sci. U. S. A. 102, 10736–10741.
Ma, Q., Ding, Y., Chang, J., Sun, X., Zhang, L., Wei, Q., Cheng, Y., Chen, L., Xu, J., Deng, X., 2014. Comprehensive insights on how 2, 4-dichlorophenoxyacetic acid retards senescence in post-harvest citrus fruits using transcriptomic and proteomic approaches. J. Exp. Bot. 65, 61–74.
Manjunatha, G., Lokesh, V., Neelwarne, B., 2010. Nitric oxide in fruit ripening: trends and opportunities. Biotechnol. Adv. 28, 489–499.
Matsumoto, H., Ikoma, Y., 2012. Effect of different postharvest temperatures on the accumulation of sugars, organic acids, and amino acids in the juice sacs of Satsuma mandarin (*Citrus unshiu* Marc.) fruit. J. Agric. Food Chem. 60, 9900–9909.
Omidbakhshfard, M.A., Omranian, N., Ahmadi, F.S., Nikoloski, Z., Mueller-Roeber, B., 2012. Effect of salt stress on genes encoding translation-associated proteins in *Arabidopsis thaliana*. Plant Signal. Behav. 7, 1095.
Osorio, S., Alba, R., Nikoloski, Z., Kochevenko, A., Fernie, A.R., Giovannoni, J.J., 2012. Integrative comparative analyses of transcript and metabolite profiles from pepper and tomato ripening and development stages uncovers species-specific patterns of network regulatory behavior. Plant Physiol. 159, 1713–1729.
Paliyath, G., Murr, D.P., Handa, A.K., Lurie, S., 2009. Postharvest Biology and Technology of Fruits, Vegetables, and Flowers. John Wiley & Sons.
Park, S., Cheng, N.H., Pittman, J.K., Yoo, K.S., Park, J., Smith, R.H., Hirschi, K.D., 2005. Increased calcium levels and prolonged shelf life in tomatoes expressing arabidopsis H+/Ca2+ transporters. Plant Physiol. 139, 1194–1206.
Porat, R., Weiss, B., Cohen, L., Daus, A., Goren, R., Droby, S., 1999. Effects of ethylene and 1-methylcyclopropene on the postharvest qualities of 'Shamouti'oranges. Postharvest Biol. Technol. 15, 155–163.
Rushton, P.J., Somssich, I.E., Ringler, P., Shen, Q.J., 2010. WRKY transcription factors. Trends Plant Sci. 15, 247–258.
Sebastià, C.H., Hardin, S.C., Clouse, S.D., Kieber, J.J., Huber, S.C., 2004. Identification of a new motif for CDPK phosphorylation in vitro that suggests ACC synthase may be a CDPK substrate. Arch. Biochem. Biophys. 428, 81–91.
Selvaraj, Y., 1993. Changes in enzymes activity in ripening pineapple fruit. Indian J. Hortic. 50, 310–317.
Sun, L., Yuan, B., Zhang, M., Wang, L., Cui, M., Wang, Q., Leng, P., 2012. Fruit-specific RNAi-mediated suppression of SlNCED1 increases both lycopene and β-carotene contents in tomato fruit. J. Exp. Bot. 63, 3097–3108.
Sun, L., Zhang, M., Ren, J., Qi, J., Zhang, G., Leng, P., 2010. Reciprocity between abscisic acid and ethylene at the onset of berry ripening and after harvest. BMC Plant Biol. 10, 257.
Sun, X., Zhu, A., Liu, S., Sheng, L., Ma, Q., Zhang, L., Nishawy, E.M.E., Zeng, Y., Xu, J., Ma, Z., 2013. Integration of metabolomics and subcellular organelle expression microarray to increase understanding the organic acid changes in post-harvest citrus fruit. J. Integr. Plant Biol. 55, 1038–1053.
Sweetman, C., Deluc, L.G., Cramer, G.R., Ford, C.M., Soole, K.L., 2009. Regulation of malate metabolism in grape berry and other developing fruits. Phytochemistry 70, 1329–1344.
Tietel, Z., Feldmesser, E., Lewinsohn, E., Fallik, E., Porat, R., 2011. Changes in the transcriptome of'Mor'Mandarin flesh during storage: emphasis on molecular regulation of fruit flavor deterioration. J. Agric. Food Chem. 59, 3819–3827.
Trapnell, C., Hendrickson, D.G., Sauvageau, M., Goff, L., Rinn, J.L., Pachter, L., 2013. Differential analysis of gene regulation at transcript resolution with RNA-seq. Nat. Biotechnol. 31, 46–53.
Trapnell, C., Pachter, L., Salzberg, S.L., 2009. TopHat: discovering splice junctions with RNA-Seq. Bioinformatics 25, 1105–1111.
Trapnell, C., Williams, B.A., Pertea, G., Mortazavi, A., Kwan, G., van Baren, M.J., Salzberg, S.L., Wold, B.J., Pachter, L., 2010. Transcript assembly and quantification by RNA-Seq reveals unannotated transcripts and isoform switching during cell differentiation. Nat. Biotechnol. 28, 511–515.
Wingler, A., Roitsch, T., 2008. Metabolic regulation of leaf senescence: interactions of sugar signalling with biotic and abiotic stress responses. Plant Biol. 10, 50–62.
Wu, J., Xu, Z., Zhang, Y., Chai, L., Yi, H., Deng, X., 2014. An integrative analysis of the transcriptome and proteome of the pulp of a spontaneous late-ripening sweet orange mutant and its wild type improves our understanding of fruit ripening in citrus. J. Exp. Bot. eru044.
Yu, Q., An, L., Li, W., 2014. The CBL–CIPK network mediates different signaling pathways in plants. Plant Cell Rep. 33, 203–214.
Yun, Z., Jin, S., Ding, Y., Wang, Z., Gao, H., Pan, Z., Xu, J., Cheng, Y., Deng, X., 2012. Comparative transcriptomics and proteomics analysis of citrus fruit, to improve understanding of the effect of low temperature on maintaining fruit quality during lengthy post-harvest storage. J. Exp. Bot. 63, 2873–2893.
Zhang, D.-P., 2014. Abscisic Acid: Metabolism, Transport and Signaling. Springer.
Zhang, L., Yu, Z., Jiang, L., Jiang, J., Luo, H., Fu, L., 2011. Effect of post-harvest heat treatment on proteome change of peach fruit during ripening. J. Proteom. 74, 1135–1149.
Zhang, L., Jiang, L., Shi, Y., Haibo, L., Kang, R., Yu, Z., 2012. Post-harvest 1-methylcyclopropene and ethephon treatments differently modify protein profiles of peach fruit during ripening. Food Res. Int. 48, 609–619.